



Transparent self-cleaning coating prepared from SiO₂/B₄C and SiO₂/B₄C/TiO₂ for the solar cell

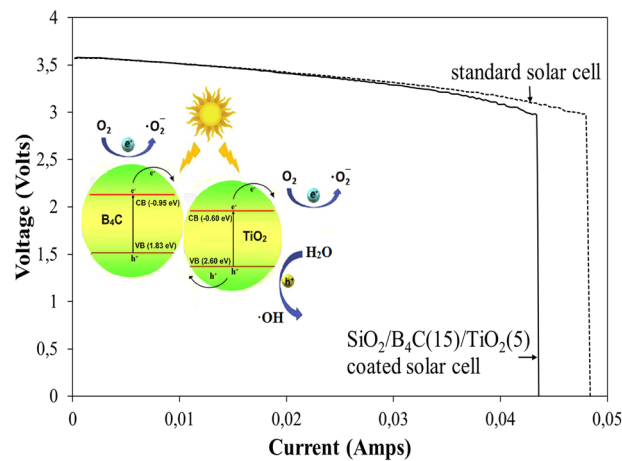
Hafize Nagehan Koysuren¹ · Ozcan Koysuren²

Received: 14 June 2024 / Accepted: 24 July 2024 / Published online: 31 July 2024
© The Author(s) 2024

Abstract

Transparent self-cleaning coatings based on photocatalytic activity have attracted great attention in recent years owing to their promising applications in many fields, such as solar cell cover glass. This study reports a simple method to prepare transparent self-cleaning silicon dioxide (SiO₂) coatings filled by boron carbide (B₄C) and titanium dioxide (TiO₂) nanoparticles. A sol-gel technique was used to synthesize a SiO₂ solution containing B₄C and TiO₂ nanoparticles, and a dip-coating technique was followed to coat the composite solution on glass slides. The SiO₂ coating was successfully obtained in the presence of both semiconductor nanoparticles as confirmed by FTIR and XRD measurements. Both the photocatalytic activity and self-cleaning property of the composite coatings were evaluated by photocatalytic degradation of a model dye, methylene blue, under visible light irradiation. The SiO₂ coating containing both B₄C and TiO₂ nanoparticles exhibited an improved photocatalytic activity compared to the SiO₂ coating including only B₄C. In particular, a 46% degradation rate of the model dye methylene blue was achieved for the SiO₂ coating containing 15 wt% B₄C and 5 wt% TiO₂ nanoparticles. Highly transparent composite coatings on glass slides were prepared. The SiO₂ coating containing both B₄C and TiO₂ nanoparticles was found to exhibit ~8% reduction in the optical transmission of the glass slide and ~1% reduction in the efficiency of a solar cell containing the coated glass slide. These findings demonstrated that the SiO₂ composite coatings have potential for self-cleaning applications in removing contaminants from the glass cover of the solar cell under visible light irradiation.

Graphical Abstract



Keywords SiO₂ · B₄C · TiO₂ · Self-cleaning coating · Photocatalytic activity

✉ Ozcan Koysuren
koysuren@ankara.edu.tr

² Department of Energy Systems Engineering, Ankara University, Ankara 06830, Turkey

¹ Department of Environmental Engineering, Kirsehir Ahi Evran University, Kirsehir 40100, Turkey

Highlights

- SiO₂ was synthesized in the presence of both B₄C and TiO₂ nanoparticles
- B₄C and TiO₂ nanoparticle did not significantly affect the light transmission and the efficiency of the solar cell
- TiO₂ enhanced the photocatalytic dye degradation efficiency of the SiO₂ coating including B₄C nanoparticles

1 Introduction

Solar energy is an inexhaustible resource that has the advantages of being renewable and clean. Solar cells are considered a powerful strategy to harness solar energy [1]. Crystalline silicon (c-Si) solar cell modules hold more than 90% of the solar cell market share. C-Si solar cell modules mainly include a front side glass cover with a thickness of 3.2 mm [2]. Within the solar cell module, the glass cover plays an important role. It serves as a vital shield, protecting the solar cell. The glass cover provides stability and rigidity for the solar cell under harsh environmental conditions. It has an important role in collecting, transmitting and reducing light reflection, all of which are beneficial to solar cell efficiency. On the other hand, the glass cover can be contaminated with dust and organic waste, resulting in scattering of incident light and reducing the efficiency of solar cells [1, 2]. The efficiency of the solar cell module that is exposed to the outdoors for a year without any cleaning is likely to decrease by up to 78% [1].

Self-cleaning is one of the most studied topics today, as it can clean the surface without the need for any external resources [3]. Maintaining the cleanliness of the glass cover of the solar cell module is a significant challenge [4]. Various self-cleaning methods such as manual, electrostatic and mechanical have been used to clean the glass cover of the solar cell. Mechanical techniques consume significant power due to moving parts [5]. Cleaning robots have attracted great attention within the scope of the mechanical techniques. But, the cleaning robots are expensive to use, and mostly require the presence of 2 to 3 operators [4]. Electrostatic techniques require significant electrical power [5]. Manual cleaning requires more labor and consumes more water. Therefore, a self-cleaning coating may be one of the best solutions to clean the glass cover [4].

Ideal coating materials for the glass cover of the solar cell should have outstanding self-cleaning properties while also maintaining high transparency. Self-cleaning coatings based on hydrophilic and hydrophobic surface properties offer viable solutions for cleaning contaminants from the glass cover of the solar cell with good reliability and affordability. The self-cleaning coatings require zero power consumption and do not corrode the glass cover of the solar cell, thus preventing any potential reduction in power production. The self-cleaning coatings can be differentiated according to their water contact behavior [5].

Hydrophobic coatings have unique self-cleaning features inspired by the lotus leaf. They are characterized by their

micro/nano-hierarchical structures, preventing dust particles and other contaminants from accumulating on the glass cover [6]. The air trapped inside the hierarchical structures maintains stable liquid-air interface with minimum solid fraction, which is in contact with water [7]. On hydrophobic coatings, water droplets can quickly roll down the surface and remove contaminants due to the water repellency of the surface [8]. Surface roughness is the most important criterion for developing hydrophobic coatings. Although the surface roughness supports the self-cleaning feature, it has a significant challenge to transparency. The surface roughness is one of the main reasons for the degradation of optical transmittance [3]. Hydrophilic self-cleaning coatings with photocatalytic activity are considered a suitable solution to remove contaminations and dust particles on the glass cover of the solar cell module [9]. On hydrophilic coatings, water droplets can quickly spread over the entire surface of the coating, forming a water film. Hence, contaminants on the surface of the coatings can be washed away during the spreading process [8]. It is also believed that the hydrophilic coating is more stable and has a longer lifespan than the superhydrophobic coating [9]. Several semiconductors like TiO₂ [9], g-C₃N₄ [10], WO₃ [11], ZnO [12] and ZrO₂ [13] have been used to obtain coatings, exhibiting both photocatalytic self-cleaning property and hydrophilicity. The hydrophilicity of the photocatalyst film can be improved upon the sunlight irradiation. The sunlight can induce surface element vacancies, and radical species can form at the surface of the coating, which can help wet the entire surface with water. Additionally, contaminants adsorbed on the photocatalyst coating can undergo oxidative decomposition upon the sunlight irradiation. During wetting of the coating surface, a water film can form, which removes both the decomposition products and contaminants. This phenomenon is known as the hydrophilic self-cleaning effect and has been found to be useful for the application of keeping the surface of the glass cover of the solar cell clean [14].

Boron carbide (B₄C) is a low-cost and stable semiconductor. It exhibits strong absorption under the sunlight due to its mid-gap states. It has a narrow optical band gap and tunable electrical properties. In addition, it has a strong oxidation resistance [15]. B₄C exhibits photocatalytic activity, outstanding physical and mechanical properties, chemical inertness, wear resistance and hydrophilic character with an initial contact angle of 61° [16, 17]. The film coating planned to be coated on the cover glass of the solar cell is expected to be unaffected by environmental conditions and to have a stable structure and hydrophilic

character. Due to the mentioned properties, B_4C may be a suitable candidate for self-cleaning coatings. However, very few studies have been reported in the literature on the photocatalytic activity and self-cleaning application of B_4C . Also, there is no study on the self-cleaning coating application of B_4C for the solar cell. In this context, Yan and his coworkers examined the photocatalyst potential of B_4C for the CO_2 reduction process [18]. As an alternative, B_4C was combined with ZnO [19], $g-C_3N_4$ [20], $Bi_7O_9I_3$ [15] and $BiOI$ [21], respectively, in a heterojunction structure and its photocatalytic activity was evaluated using dye degradation, hydrogen production and CO_2 reduction processes.

However, the high refractive index and narrow band gap of B_4C causes high reflectance and absorbance, which can lower the efficiency of the solar cell module. To minimize the absorption of the glass cover of the solar cell, the optical band gap of the self-cleaning coating should be wide enough to reduce the absorption loss in the visible light spectrum of the sunlight. Moreover, to minimize the reflection of the glass cover of the solar cell, the refractive index of self-cleaning coating should be close to the refractive index of the glass cover (1.21–1.25) [9]. In the literature, SiO_2 , helping in the reduction of the refractive index of the composite structure, was combined with TiO_2 [7, 22], ZnO [22], ZrO_2 [23], Fe_2O_3 [24] and graphene oxide [24], respectively, to form transparent coatings. Combining the semiconductor photocatalyst with SiO_2 can enhance the visible light transmission owing to the wide band gap and the suitable refractive index of SiO_2 . Additionally, SiO_2 can improve both the chemical durability and mechanical properties of coatings. SiO_2 can make the coating more adherent and robust, increasing the application potential of the self-cleaning coating on the glass cover of the solar cell module [8].

In this study, B_4C was combined with SiO_2 in the solution phase and coated on a glass slide using a dip coating method. The effect of B_4C content in SiO_2/B_4C coatings on the light transmittance and the solar cell efficiency was studied. From the practical point of view, a good self-cleaning coating for the glass cover of the solar cell module should have both high transmittance and high photocatalytic activity. TiO_2 has been known as an efficient photocatalyst under the sunlight. Among various photocatalysts, TiO_2 has attracted great attention due to its high photocatalytic activity, physical and chemical stability, low cost and environmentally benign [8]. To enhance the photocatalytic activity of the SiO_2/B_4C coating, TiO_2 was combined with SiO_2 in the solution phase. TiO_2 has a wide band gap (e.g. ≈ 3.20 eV) but also a large refractive index ($n \approx 2.52$ for anatase). Therefore, it can only absorb a small part of the sunlight, but can reflect a certain part of the sunlight [8, 14]. An attempt has been made to enhance the photocatalytic activity of SiO_2/B_4C coatings by adding TiO_2 without reducing the light transmittance of the glass cover of the solar

cell and the efficiency of the solar cell including the coated glass cover too much. Organic pollutants on the coating surface could be removed by the synergistic photocatalytic performance of B_4C and TiO_2 in the SiO_2 phase. Therefore, the prepared coating exhibited a self-cleaning property. While this study enabled the development of self-cleaning coatings, it did not significantly affect the efficiency of the solar cell on which it was applied. This study provided a new perspective for the synergistic application of B_4C and TiO_2 in the field of self-cleaning coatings for solar cells.

2 Experimental

2.1 Materials and methods

SiO_2 coatings on glass slides were prepared from a SiO_2 solution using a simple dip coating technique. The SiO_2 solution was prepared by a sol-gel process of tetraethylorthoxysilicane (TEOS) using hydrochloric acid (HCl) as catalyst. 112 ml of TEOS was added into a certain amount of distilled water-anhydrous ethanol solution (36–1090 ml). As-prepared solution was kept at constant stirring at the room temperature. Then, a certain amount of HCl (~ 0.2 ml, 36%) was added into the as-prepared solution to obtain a final solution. Afterward, B_4C nanoparticles (40–60 nm, Nanografi) were added into the prepared SiO_2 solution and it was kept at stirring for 1 day to obtain a uniform coating solution of SiO_2/B_4C . The B_4C content of the composite solution was adjusted to be 5, 10 and 15 wt.%, respectively. The composite coating solutions were labeled as $SiO_2/B_4C(100-x/x)$ ($x = 5, 10, 15$), respectively. In addition, TiO_2 nanoparticles (< 25 nm, Sigma-Aldrich) were also dispersed in the prepared SiO_2/B_4C solution to obtain a $SiO_2/B_4C/TiO_2$ solution. TiO_2 was added into the $SiO_2/B_4C(15)$ solution and the TiO_2 content of the final solution was adjusted to be 5 wt.%. The composite solution was labeled as $SiO_2/B_4C(15)/TO_2(5)$. Before the dip coating process, ultrasonic cleaning was applied to the glass slides. The composite solutions were coated on the glass slides through the dip-coating method. The glass slides were dried at the ambient condition for 2 h and then they were dried at $100^\circ C$ for 1 h to remove the unreacted volatile species. Finally, the coated glass slides were annealed at $400^\circ C$ for 2 h [25].

2.2 Structural, morphological and optical characterization

To study the morphology of the composite coatings, optical microscopy images and field emission scanning electron microscopy (FESEM) images were obtained on a LEICA model binocular microscope and on a QUANTA 400F model microscope, respectively. The UV-Vis absorbance and transmittance spectra of the composite coatings were recorded

by a Genesys 10S (Thermo Scientific) model spectrophotometer in the absorbance mode and transmittance mode, respectively. The FTIR spectra of the samples were recorded using a Bruker IFS 66/S model spectrophotometer with a resolution of 4 cm^{-1} . X-ray diffraction (XRD) patterns of the composite coatings were recorded by a Rigaku Ultima IV model diffractometer with Cu-K α radiation at a scan rate of $1^\circ/\text{min}$. The efficiency of the solar cell including coated glass slides and the solar cell including uncoated glass slide (standard) was compared using a PROVA 210 model solar module analyzer. The efficiency of the solar cell was calculated using the following relation [26]:

$$\eta(\text{efficiency}) = V_{\text{OC}} I_{\text{SC}} \text{FF} / P_{\text{in}} \quad (1)$$

where V_{OC} is the open-circuit voltage (V), I_{SC} is the short-circuit current (A), FF is the fill factor and P_{in} is the incident radiation flux (W/m^2). The fill factor was calculated by using the following relation [26]:

$$\text{FF} = V_{\text{MP}} I_{\text{MP}} / V_{\text{OC}} I_{\text{SC}} \quad (2)$$

where V_{MP} and I_{MP} are the voltage value (V) and the current value (A), respectively, at the maximum power point.

The water contact angle measurement of the coating samples was performed using an optical tensiometer (Theta Lite, Biolin Scientific) at 3 different points and the average of these measurement was reported in the manuscript.

2.3 Characterization of the photocatalytic performance

The photocatalytic activity of the composite coatings was evaluated by photodegradation of a model dye, methylene blue. In a flat glass container, 50 ml of aqueous methylene blue solution (10 mg/l) was added and the coated glass slides were immersed into the dye solution. To attain the adsorption-desorption equilibrium between the dye molecules and the coatings, the samples was kept in the solution for 30 min before the visible light irradiation. Then the dye solution including the coated glass slide was exposed to the visible light irradiation using a 300 W lamp (Osram Ultravitalux). 2 ml of the dye solution was withdrawn from the solution including the coated glass slide at regular interval of time (60 min) and the sample solution was analyzed using the Genesys 10S (Thermo Scientific) model spectrophotometer. The percentage of the photocatalytic degradation of methylene blue was calculated using the following relation:

$$\% \text{Degradation of methylene blue} = (C_0 - C) / C_0 \times 100 \quad (3)$$

at which C_0 and C are the solution concentrations before the visible light irradiation and after the visible light irradiation, respectively [27].

3 Results and discussion

3.1 FTIR analysis

On the FTIR spectrum of the $\text{SiO}_2/\text{B}_4\text{C}(15)$ coating (Fig. 1a), there are absorption peaks of the anti-symmetric and symmetric vibrations of the Si-O-Si bond at 1193 and 812 cm^{-1} , respectively. The absorption peak at 453 cm^{-1} reflects the flexural vibration of the Si-O-Si bond. The wide absorption band at around 3205 cm^{-1} and the weak absorption peak at 1739 cm^{-1} correspond to the stretching and bending vibrations of the hydroxyl groups on the $\text{SiO}_2/\text{B}_4\text{C}(15)$ coating [28]. On the same spectrum, the weak absorption peak at 640 and 1076 cm^{-1} are attributed to the weak vibrations of the B-B bond of B_4C . The peak at 1193 cm^{-1} can also be attributed to the B-C bonds in the icosahedra. In addition, the absorption peak at 1380 cm^{-1} is assigned to the disordered graphite structure of B_4C [29]. On the FTIR spectrum of the $\text{SiO}_2/\text{B}_4\text{C}(15)/\text{TiO}_2(5)$ coating (Fig. 1b), there are absorption peaks at 812 and 453 cm^{-1} belonging to the symmetric vibration of Si-O-Si and the flexural vibration of Si-O-Si bond, respectively [28]. The intense peak at 1194 cm^{-1} can be attributed to both the anti-symmetric vibration of Si-O-Si bond and the B-C bonds in the icosahedra. The peaks belonging to the weak vibrations of the B-B bond are present at 635 and 1074 cm^{-1} . The peak due to the disordered graphite structure of B_4C is present 1378 cm^{-1} [29]. In addition to the peaks belonging to SiO_2 and B_4C chemical structures, there is an absorption band at around 538 cm^{-1} due to the Ti-O-Ti bond [28]. FTIR spectrum of the $\text{SiO}_2/\text{B}_4\text{C}(15)$ and the $\text{SiO}_2/\text{B}_4\text{C}(15)/\text{TiO}_2(5)$ coatings confirmed the successful synthesis of SiO_2 coating in the presence of B_4C and TiO_2 nanoparticles.

3.2 XRD analysis

Figure 2 illustrates the X-ray diffractogram of the $\text{SiO}_2/\text{B}_4\text{C}(15)$ and $\text{SiO}_2/\text{B}_4\text{C}(15)/\text{TiO}_2(5)$ coatings. There is an

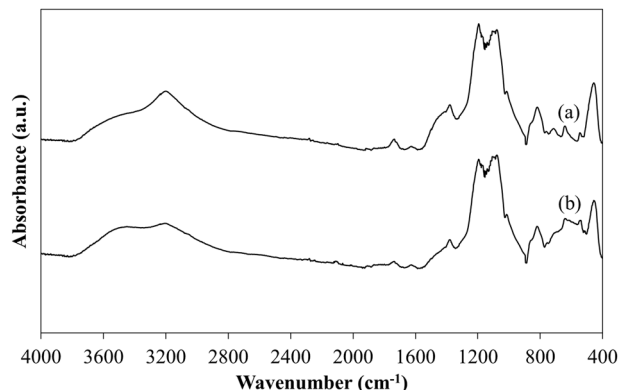


Fig. 1 FTIR spectrum of (a) $\text{SiO}_2/\text{B}_4\text{C}(15)$ and (b) $\text{SiO}_2/\text{B}_4\text{C}(15)/\text{TiO}_2(5)$ coatings

intense band on the X-ray diffractogram of both samples at around $2\theta = 22^\circ$, corresponding to the amorphous SiO_2 [30]. The X-ray diffractogram of the $\text{SiO}_2/\text{B}_4\text{C}(15)$ coating also exhibits the existence of peaks at $2\theta = 22.1^\circ, 23.4^\circ, 31.9^\circ, 35.0^\circ, 37.7^\circ$ and 53.3° assigned to (003), (012), (110), (104), (021) and (205) crystal planes of the rhombohedral B_4C (Fig. 2a) [31]. When $\text{SiO}_2/\text{B}_4\text{C}$ was combined with TiO_2 , a small shift in the 2θ of the diffraction peaks of B_4C was observed. The characteristic peaks of B_4C are present at $2\theta = 22.2^\circ, 23.5^\circ, 31.9^\circ, 34.9^\circ, 37.8^\circ$ and 53.3° corresponding to (003), (012), (110), (104), (021) and (205) crystal planes of B_4C (Fig. 2b) [31]. There are weak peaks at $2\theta = 25.4^\circ, 39.2^\circ$ and 48.2° on the diffractogram of the $\text{SiO}_2/\text{B}_4\text{C}(15)/\text{TiO}_2(5)$ coating, assigned to the (101), (004) and (200) crystal planes of TiO_2 in anatase form (Fig. 2b) [30].

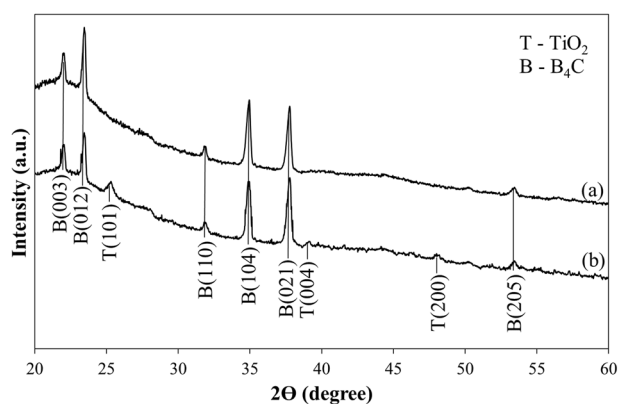
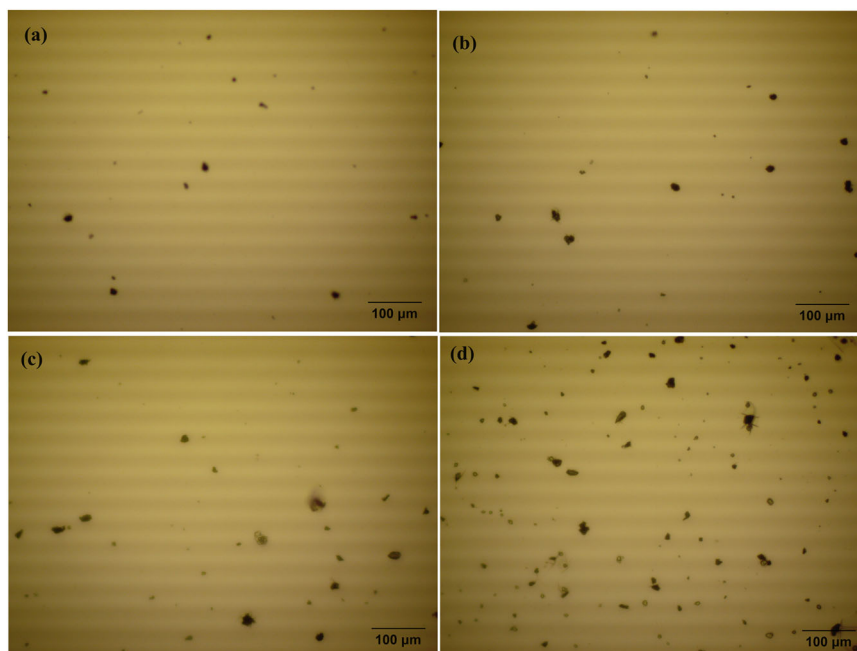


Fig. 2 XRD pattern of (a) $\text{SiO}_2/\text{B}_4\text{C}(15)$ and (b) $\text{SiO}_2/\text{B}_4\text{C}(15)/\text{TiO}_2(5)$ coatings

Fig. 3 Optical microscopy image of (a) $\text{SiO}_2/\text{B}_4\text{C}(5)$, (b) $\text{SiO}_2/\text{B}_4\text{C}(10)$, (c) $\text{SiO}_2/\text{B}_4\text{C}(15)$ and (d) $\text{SiO}_2/\text{B}_4\text{C}(15)/\text{TiO}_2(5)$ coatings



3.3 Morphology analysis

Figure 3 illustrates optical micrographs of the composite coatings at various B_4C and TiO_2 contents. The $\text{SiO}_2/\text{B}_4\text{C}(5)$ coating includes small islands irregular in size and shape (Fig. 3a). As the B_4C content of the coating increases, the number and the size of the islands slightly increase. According to the optical microscope images, B_4C nanoparticles tended to agglomerate. However, it was observed that the B_4C agglomerate structures were dispersed homogeneously (Fig. 3a–c). Figure 3d shows the optical microscopy image of the $\text{SiO}_2/\text{B}_4\text{C}(15)/\text{TiO}_2(5)$ coating. There are two different island structures. Small-sized and large-sized islands may belong to TiO_2 nanoparticles and B_4C nanoparticles, respectively. Both TiO_2 and B_4C nanoparticles are homogeneously dispersed in the SiO_2 phase. According to Fig. 3, smooth and crack-free film surfaces were obtained. The FESEM images of the composite coatings are illustrated in Fig. 4. FESEM images also confirmed that B_4C and TiO_2 nanoparticles were evenly dispersed in the SiO_2 phase. Nano-hierarchical particle structures of TiO_2 and B_4C on the coating films can be seen on both images.

3.4 Optical property analysis

As shown in Fig. 5, the $\text{SiO}_2/\text{B}_4\text{C}$ and $\text{SiO}_2/\text{B}_4\text{C}/\text{TiO}_2$ coatings exhibited absorption mainly in the UV light region due to the wide band gap SiO_2 . When the B_4C content of $\text{SiO}_2/\text{B}_4\text{C}$ coatings increased, the optical absorption of the coatings in the region of 200–800 nm did not change

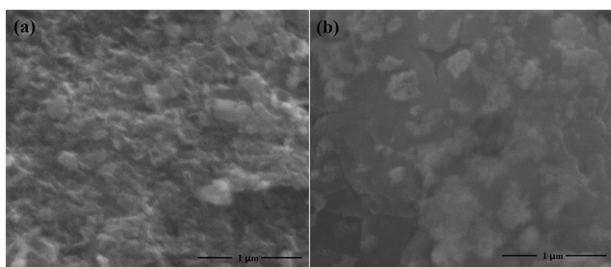


Fig. 4 FESEM image of (a) SiO₂/B₄C(15) and (b) SiO₂/B₄C(15)/TiO₂(5) coatings

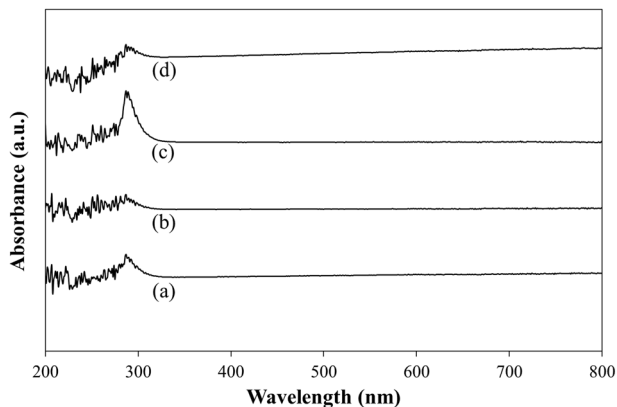


Fig. 5 UV-Vis absorption spectrum of (a) SiO₂/B₄C(5), (b) SiO₂/B₄C(10), (c) SiO₂/B₄C(15) and (d) SiO₂/B₄C(15)/TiO₂(5) coatings

significantly. Moreover, combining the SiO₂/B₄C coating with TiO₂ did not have a significant effect on the absorption. Low light absorption in the visible light region is very important for the efficiency of the solar cell. The optical band gap (E_g) of the composite coatings can be estimated from the following relationship using the UV-Vis absorbance data [32]:

$$(\alpha h\nu)^2 = A(h\nu - E_g) \quad (4)$$

where α is the absorption coefficient, $h\nu$ is the photon energy, A is a proportionality constant and E_g is the optical band gap, respectively. As shown in Supplementary Fig. S1, the band gap of the SiO₂/B₄C(5), SiO₂/B₄C(10), SiO₂/B₄C(15) and SiO₂/B₄C(15)/TiO₂(5) coatings is 4.1 eV, 4.0 eV, 4.0 eV and 3.8 eV, respectively. In addition, the optical band gap of pure SiO₂, pure B₄C and pure TiO₂ is 4.9 eV, 2.1 eV and 2.8 eV, respectively (Supplementary Fig. S2). The band gap of a composite material depends not only on the properties of its components but also on the size, morphology and arrangement of its components. Therefore, there are many variables that affect the band gap characteristic of a composite structure. Compared to pure SiO₂ coating, there was a reduction in the band gap energy of the composite coating. The decrease in the optical band gap might indicate an increase in crystal quality which was

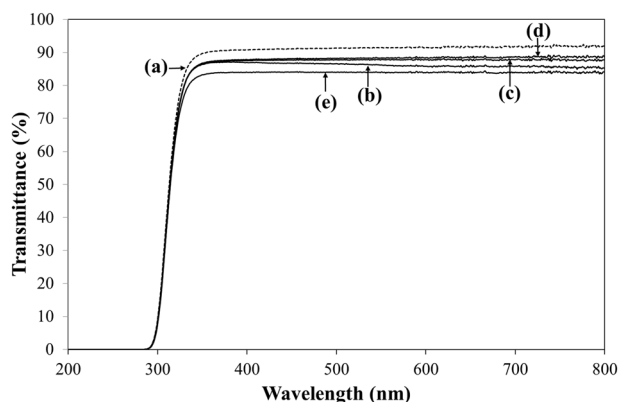


Fig. 6 UV-Vis transmission spectrum of (a) uncoated glass slide (standard) and glass slide coated with (b) SiO₂/B₄C(5), (c) SiO₂/B₄C(10), (d) SiO₂/B₄C(15), (e) SiO₂/B₄C(15)/TiO₂(5) coatings

more ordered [33]. The estimated band gap values of the composite coatings existed in the UVA region (315–400 nm) and UVB region (280–315 nm). The specified light range falls within the broad spectrum of the sunlight and close to the visible light region. This finding showed that the composite coatings can be activated under the sunlight as a photocatalyst and they allow a significant portion of the sunlight to pass through the glass cover of the solar cell into its absorber layer, which is important for the self-cleaning feature of the coatings and the efficiency of the solar cell on which the coatings are deposited.

The optical transmission of glass slides coated with the SiO₂ composite coatings was observed by UV-visible spectroscopy (Fig. 6). For comparison purpose, the optical transmission of glass slides coated with pure SiO₂, pure B₄C and pure TiO₂ was also analyzed (Supplementary Fig. S3). The average transmittance of the uncoated glass plate (standard) was 91.56% in the wavelength range of the visible light region (400–800 nm) (Fig. 6a). Compared with the uncoated standard, glass slides coated with pure SiO₂ and with the SiO₂ composites exhibited almost similar light transmittance in the visible light region. The average transmittance of the glass slide coated with SiO₂/B₄C(5), SiO₂/B₄C(10), SiO₂/B₄C(15) and SiO₂/B₄C(15)/TiO₂(5) was 86.06, 87.82, 88.44 and 83.96%, respectively (Fig. 6b–d). On the other hand, the average transmittance of the glass slide coated with pure SiO₂, pure B₄C and pure TiO₂ was 92.41, 13.09 and 11.50%, respectively (Supplementary Fig. S3a–c). Although the light transmittance of pure B₄C and pure TiO₂ is low, relatively high light transmittance was obtained in the composite structure (Supplementary Fig. S3 and Fig. 6). SiO₂ formed the main phase in all composite coatings and it might dominate the light transmittance. Figure 6 illustrates that the transmittance increased slightly with increasing the B₄C content of the SiO₂/B₄C composite coating. Compared with the SiO₂/B₄C composites, the light transmission of the glass slide coated

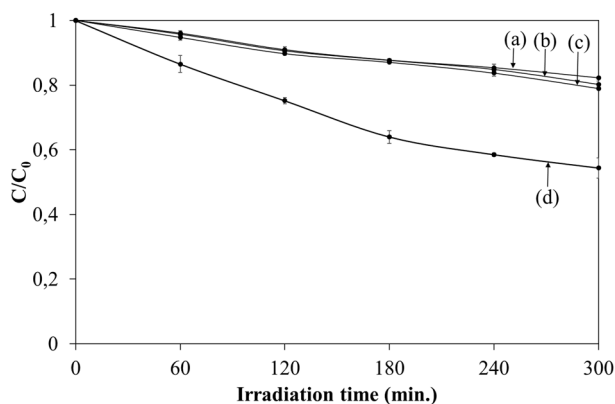


Fig. 7 The photocatalytic performance of (a) $\text{SiO}_2/\text{B}_4\text{C}(5)$, (b) $\text{SiO}_2/\text{B}_4\text{C}(10)$, (c) $\text{SiO}_2/\text{B}_4\text{C}(15)$ and (d) $\text{SiO}_2/\text{B}_4\text{C}(15)/\text{TiO}_2(5)$ coatings under visible light irradiation

with the $\text{SiO}_2/\text{B}_4\text{C}/\text{TiO}_2$ composite slightly decreased (Fig. 6e), because TiO_2 microspheres might induce an increase in the roughness of the glass surface, which enhanced the light scattering. In addition, TiO_2 due to its high refractive index might increase the light reflection. In the case of solar cells, the optical transmittance of the self-cleaning coating is extremely important, so it is desirable that the optical transmittance be the same or close to the glass cover of the solar cell itself.

3.5 Photocatalytic performance

Supplementary Fig. S4 exhibits the UV-Vis spectra of methylene blue in the presence of composite coatings under visible light irradiation. After exposure to the visible light, the spectral characteristic region for methylene blue reduced slightly in the presence of the $\text{SiO}_2/\text{B}_4\text{C}$ composite coatings, while its reduction is relatively strong in the presence of the $\text{SiO}_2/\text{B}_4\text{C}(15)/\text{TiO}_2(5)$ coating. After 300 min of visible light irradiation (Fig. 7a), nearly 82% of methylene blue remained in the solution in the presence of the $\text{SiO}_2/\text{B}_4\text{C}(5)$ coating. In the presence of the $\text{SiO}_2/\text{B}_4\text{C}(10)$ coating, about 80% of the model dye remained in the solution after 300 min of visible light irradiation (Fig. 7b). This value decreased to only about 79% in the presence of the $\text{SiO}_2/\text{B}_4\text{C}(15)$ coating (Fig. 7c). The results exhibited that the photocatalytic dye degradation efficiency of the $\text{SiO}_2/\text{B}_4\text{C}$ coatings was low. No significant increase in the photocatalytic dye degradation efficiency was observed with an increase in the B_4C content of the coatings. To enhance the photocatalytic activity, the $\text{SiO}_2/\text{B}_4\text{C}$ coating was combined with a well-known photocatalyst TiO_2 . After 300 min of visible light irradiation (Fig. 7d), nearly 54% of methylene blue remained in the solution in the presence of the $\text{SiO}_2/\text{B}_4\text{C}(15)/\text{TiO}_2(5)$ coating. In other words, almost 46% of the model dye was degraded at 300 min. The results indicated

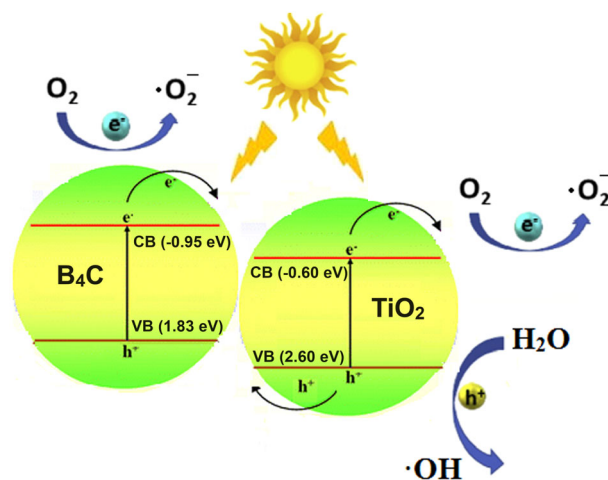


Fig. 8 The proposed photocatalytic degradation mechanism on the $\text{B}_4\text{C}-\text{TiO}_2$ heterojunction structure within the SiO_2 coating

that the $\text{SiO}_2/\text{B}_4\text{C}(15)/\text{TiO}_2(5)$ coating possesses higher photocatalytic activity than that of the $\text{SiO}_2/\text{B}_4\text{C}$ coatings. Figure 8 exhibits the proposed energy band structure and the photocatalytic degradation mechanism on $\text{B}_4\text{C}/\text{TiO}_2$ [21, 34]. According to the study of Bledowski and his coworkers, the conduction band and the valence band values of TiO_2 were used as -0.60 eV and 2.60 eV, respectively [34]. In addition, the conduction band (-0.95 eV) and the valence band (1.83 eV) values of B_4C were taken from the study of Lv and his coworkers [21]. When the $\text{SiO}_2/\text{B}_4\text{C}(15)/\text{TiO}_2(5)$ coating absorbs the visible light with photon energy equal or higher than the band gap of B_4C and/or TiO_2 , the valence band electrons could be excited to the conduction band of the composite constituents, leading to the formation of photoinduced holes in the valence band and photoinduced electrons in the conduction band. Due to the difference in the band energies, combining B_4C and TiO_2 in the SiO_2 coating could cause electrons to move from the conduction band of B_4C to the conduction band of TiO_2 . Meanwhile, the valence band electrons of TiO_2 could move to the valence band of B_4C [21, 34]. The electrostatic field between B_4C and TiO_2 in the SiO_2 film might force the photoexcited electron-hole pairs to separate, preventing the recombination of the photoexcited charge carriers to some extent (Fig. 8). The photoinduced charge carriers could participate in the photocatalytic dye degradation reactions. The estimated potential of photoinduced electrons (-0.95 eV (B_4C) & -0.60 eV (TiO_2) vs. NHE) allows for photoreduction of surface adsorbed oxygen molecules (-0.33 eV vs. NHE) to superoxide radicals, and the estimated potential of photoinduced holes (2.60 eV (TiO_2) vs. NHE) allows for photooxidation of surface adsorbed water molecules (2.27 eV vs. NHE) to hydroxyl radicals (Fig. 8) [21, 34]. In addition, the estimated potential of photoinduced electrons of both B_4C

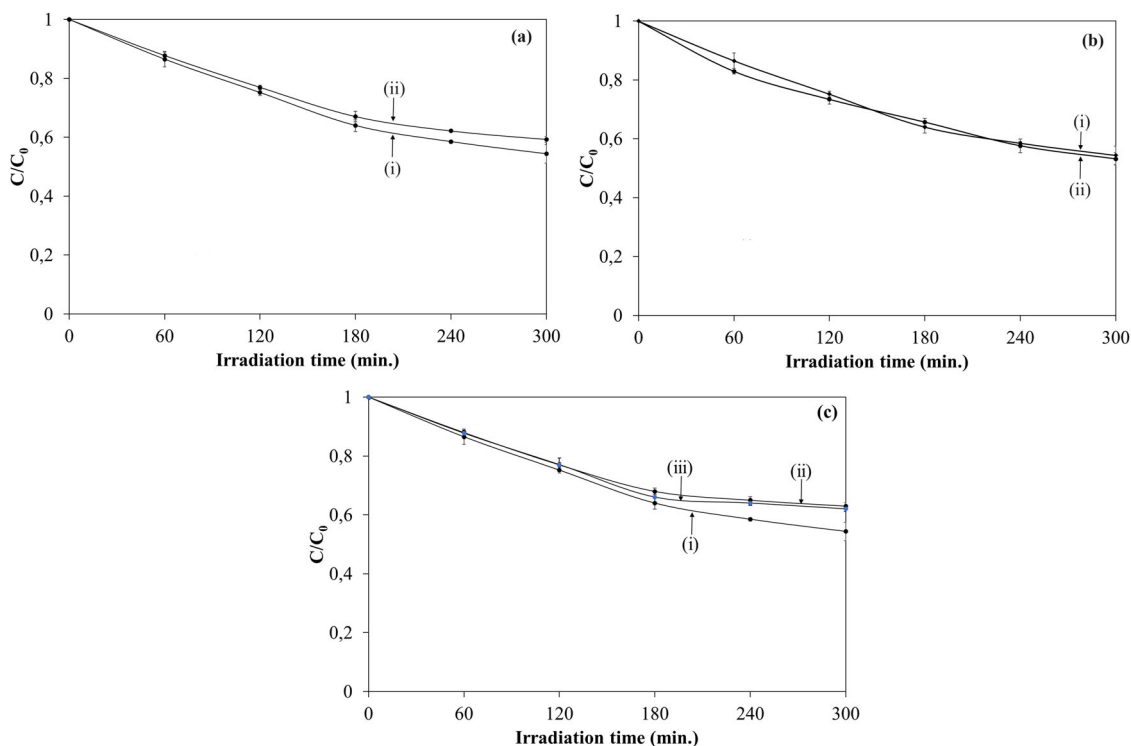


Fig. 9 **a** The photocatalytic performance of (i) $\text{SiO}_2/\text{B}_4\text{C}(15)/\text{TiO}_2(5)$, (ii) $\text{SiO}_2/\text{TiO}_2(5)$; **b** The photocatalytic performance of (i) $\text{SiO}_2/\text{B}_4\text{C}(15)/\text{TiO}_2(5)$ coating under visible light irradiation, (ii) $\text{SiO}_2/\text{B}_4\text{C}(15)/\text{TiO}_2(5)$ coating under UVA light irradiation; **c** The

photocatalytic performance of the $\text{SiO}_2/\text{B}_4\text{C}(15)/\text{TiO}_2(5)$ coating (i) in the absence of a radical scavenger, (ii) in presence of tert-butanol (hydroxyl radical scavenger), (iii) in presence of ascorbic acid (superoxide radical scavenger)

and TiO_2 allows for photoreduction superoxide radicals to hydrogen peroxide (0.69 eV vs. NHE) and then hydroxyl radicals (0.38 eV vs. NHE) [35]. Therefore, the photo-generated electrons of TiO_2 and the photoinduced electrons transferred from the conduction band of B_4C could convert the surface adsorbed oxygen to superoxide radicals directly or the superoxide radicals to hydroxyl radicals indirectly. Meanwhile, the photogenerated electrons remained in the conduction band of B_4C and the photogenerated holes remained in the valence band of TiO_2 might cause the transformation of surface adsorbed oxygen into superoxide radicals and surface adsorbed water into hydroxyl radicals, respectively. It should be the reason for the enhancement in the photocatalytic dye degradation efficiency observed with the $\text{SiO}_2/\text{B}_4\text{C}(15)/\text{TiO}_2(5)$ coating [21, 34].

The superoxide and hydroxyl radicals are strong active species, able to degrade organic contaminant accumulated on the glass cover of the solar cell into harmless small molecules, which is the basis of the self-cleaning mechanism expected under the sunlight. When compared with the $\text{SiO}_2/\text{B}_4\text{C}$ coatings, there was a significant enhancement in the photocatalytic dye degradation efficiency of the the $\text{SiO}_2/\text{B}_4\text{C}(15)/\text{TiO}_2(5)$ coating. To be sure whether the reason for this improvement is the presence of the well-known photocatalyst TiO_2 or the heterojunction structure between $\text{B}_4\text{C}-\text{TiO}_2$, the photocatalytic dye degradation

experiment in the presence of the $\text{SiO}_2/\text{TiO}_2$ coating was also performed. After 300 min of visible light irradiation (Fig. 9a), nearly 59% of methylene blue remained in the solution in the presence of the $\text{SiO}_2/\text{TiO}_2(5)$ coating. It supported the idea that the heterojunction structure between B_4C and TiO_2 in the SiO_2 film provided the enhancement in the photocatalytic dye degradation efficiency. To examine the effect of the light source on the photocatalytic dye degradation, a UVA (12 W) light source was also tried as an alternative to the visible light source in the photocatalytic activity experiment with the $\text{SiO}_2/\text{B}_4\text{C}(15)/\text{TiO}_2(5)$ coating. At the end of 300 min, approximately similar dye degradation values were obtained with both light sources separately (Fig. 9b), which indicated that the light source did not have a significant effect on the photocatalytic activity of the composite coating.

To reveal the exact role of hydroxyl and superoxide radicals in the photocatalytic degradation of the model dye, tert-butanol as a hydroxyl radical scavenger and ascorbic acid as a superoxide radical scavenger were added into the methylene blue solution in the presence of the $\text{SiO}_2/\text{B}_4\text{C}(15)/\text{TiO}_2(5)$ coating. It was observed that nearly 63% of methylene blue remained in the solution in the presence of tert-butanol with the $\text{SiO}_2/\text{B}_4\text{C}(15)/\text{TiO}_2(5)$ coating. On the other hand, nearly 62% of the model dye remained in the presence of ascorbic acid with the $\text{SiO}_2/\text{B}_4\text{C}(15)/\text{TiO}_2(5)$ coating (Fig. 9c). The

degree of degradation of methylene blue decreased from 46% to 37% and 38% in the presence of tert-butanol and ascorbic acid, respectively. Both types of the radical scavengers decreased the photocatalytic dye degradation ratio. According to the radical scavenger analysis, both hydroxyl and superoxide radicals played an active role in the photocatalytic dye degradation reactions.

With a hydrophilic coating, water droplets spread spontaneously over the surface of the coating, leading to the removal of the dirt and other contaminants. Additionally, the hydrophilic coatings including a suitable photocatalyst have an additional feature of decomposing the complex organic contaminants by a sunlight-assisted cleaning mechanism. Thus, the self-cleaning process can be assigned to the rainfall driven mechanism and/or the sunlight driven (photocatalytic) mechanism. Mostly, the self-cleaning process results from a combination of these two effects [36, 37]. Water contact angle measurement was also performed to investigate the hydrophilic feature of the prepared coatings. The water contact angle of pure SiO₂ coating was found to be 36.7° and it increased to 42.2° and 58.4° with the SiO₂/B₄C(15) coating and the SiO₂/B₄C(15)/TiO₂(5) coating, respectively (Supplementary Figs. S6 and S7). Comparing all the coating samples, the composite coatings exhibited higher water contact angle value. The reason for the increase in the water

contact angle value might be owing to an increase in the surface roughness of the SiO₂ film with B₄C and TiO₂.

3.6 Solar cell efficiency

To evaluate the application potential, glass slides coated with the prepared coatings were placed on top of a real solar cell and their photovoltaic performance were evaluated. The photovoltaic performance of the solar cell was investigated under visible light irradiation at an intensity of 1170 W/m². Figure 10 shows the current-voltage curves of coated and uncoated solar cells. The standard solar cell in the absence of the as-prepared coating has an efficiency (η) of 7.60% and a fill factor (FF) of 0.827 (Table 1). There was a slight decrease in both the efficiency and the fill factor, which might be due to the absorption effect of the as-prepared coatings with B₄C and TiO₂ (Table 1). According to the optical band gap calculations (Supplementary Fig. S1), the SiO₂/B₄C and SiO₂/B₄C/TiO₂ coatings could absorb a slight portion of the visible light below 309 nm and 326 nm, respectively. Among the SiO₂/B₄C coatings, there was a slight increase in the solar cell efficiency with the B₄C content, which might be due to the antireflection effect of the B₄C phase. The transmittance data also supported the opinion (Fig. 6). The SiO₂ coating with the highest B₄C content provided the highest light transmittance. Combining the SiO₂/B₄C coating with TiO₂ slightly reduced the solar cell efficiency (Table 1).

The fill factor (FF) is one of the important parameters quantifying the performance of solar cells. It is directly proportional to the power conversion efficiency of the solar cell [38]. Relatively high fill factor values were obtained with the prepared coatings. As a result of the efficiency comparison, it can be concluded that the SiO₂/B₄C and SiO₂/B₄C/TiO₂ coatings are promising candidates for the solar cell due to the low deterioration in its efficiency.

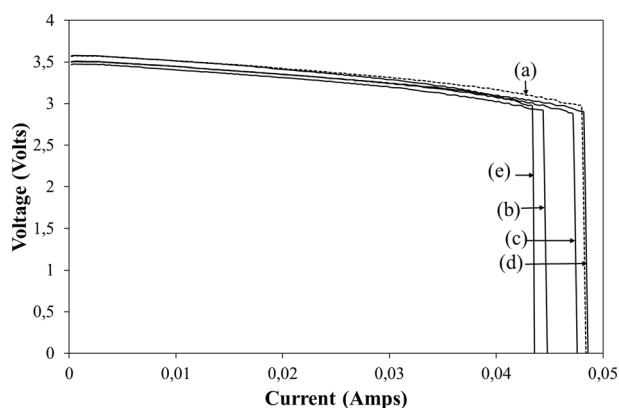


Fig. 10 Current-voltage characteristics of solar cell with (a) an uncoated glass slide (standard) and coated glass slides including (b) SiO₂/B₄C(5), (c) SiO₂/B₄C(10), (d) SiO₂/B₄C(15), (e) SiO₂/B₄C(15)/TiO₂(5) coatings

4 Conclusion

In summary, it was presented a simple technique to prepare a transparent self-cleaning coating through the synthesis of SiO₂ in the presence of B₄C and TiO₂ nanoparticles. The

Table 1 Efficiency of the solar cell including uncoated glass slide (standard) and coated glass slides

Sample	V _{MP} (V)	I _{MP} (A)	V _{oc}	I _{sc}	FF	A (m ²)	P _{out} (W/m ²)	P _{in} (W/m ²)	η (%)
Standard	2.965	0.048	3.583	0.048	0.827	0.0016	89.0	1170	7.60
SiO ₂ /B ₄ C(5)	2.915	0.044	3.484	0.045	0.818	0.0016	80.2	1170	6.85
SiO ₂ /B ₄ C(10)	2.910	0.047	3.521	0.048	0.809	0.0016	85.5	1170	7.31
SiO ₂ /B ₄ C(15)	2.895	0.048	3.512	0.049	0.807	0.0016	86.9	1170	7.42
SiO ₂ /B ₄ C(15)/TiO ₂ (5)	2.968	0.043	3.591	0.044	0.808	0.0016	79.8	1170	6.81

coated glass slides exhibited more than 83% transmittance in the wavelength range of the visible light region. Additionally, the prepared composite coatings exhibited photocatalytic activity under visible light, which is a prerequisite for the self-cleaning feature of the coating. The photocatalytic dye degradation in the presence of the composite coating reached 46% after 300 min of visible light irradiation. On the basis of this study, the prepared $\text{SiO}_2/\text{B}_4\text{C}/\text{TiO}_2$ composite coating is a potential photocatalyst for degradation of contaminants under visible light irradiation. The composite coatings did not significantly affect the efficiency of the solar cell on which the coated glass slide was placed. As a conclusion, the prepared composite coatings with both transparency and photocatalytic activity may be useful for the glass cover of the solar cell module.

Supplementary information The online version contains supplementary material available at <https://doi.org/10.1007/s10971-024-06505-7>.

Author contributions All authors contributed to the study conception and design. Material preparation, data collection and analysis were performed by Hafize Nagehan Koysuren and Ozcan Koysuren.

Funding Open access funding provided by the Scientific and Technological Research Council of Türkiye (TÜBİTAK).

Compliance with ethical standards

Conflict of interest The authors declare no competing interests.

Publisher's note Springer Nature remains neutral with regard to jurisdictional claims in published maps and institutional affiliations.

Open Access This article is licensed under a Creative Commons Attribution 4.0 International License, which permits use, sharing, adaptation, distribution and reproduction in any medium or format, as long as you give appropriate credit to the original author(s) and the source, provide a link to the Creative Commons licence, and indicate if changes were made. The images or other third party material in this article are included in the article's Creative Commons licence, unless indicated otherwise in a credit line to the material. If material is not included in the article's Creative Commons licence and your intended use is not permitted by statutory regulation or exceeds the permitted use, you will need to obtain permission directly from the copyright holder. To view a copy of this licence, visit <http://creativecommons.org/licenses/by/4.0/>.

References

- Peng J, Ye P, Xu F, Geng H, Wang R, Jiang Y, Zhu Y, Wang H (2023) Highly transparent, durable, and omniphobic liquid-like coatings for efficient dynamic de-wetting and self-cleaning applications. *Chem Eng J* 477:147090
- Tachibana T, Shirasawa K, Tanahashi K (2023) Development of lightweight and flexible crystalline silicon solar cell modules with PET film cover for high reliability in high temperature and humidity conditions. *Sol Energy Mater Sol Cells* 262:112541
- Lathe SS, Sutar RS, Kodag VS, Bhosale AK, Kumar AM, Sadasivuni KK, Xing R, Liu S (2019) Self-cleaning superhydrophobic coatings: Potential industrial applications. *Prog Org Coat* 128:52–58
- Younas M, Khan A, Amjad D, Rehman MA, Farhad AN, Mehmood U (2024) Development of robust polyvinylidene fluoride (PVDF)-based self-clean coating for commercial solar cells/panels employing spray method. *Mater Lett* 355:135486
- Rajbahadur YN, Kumar A, Negi S, Kar S (2024) Evaluation of hydrophobic/hydrophilic and antireflective coatings for photovoltaic panels. *J Coat Technol Res* 3:1–38
- Sathya RA, Ponraj C (2024) Superhydrophobic route of fabricating antireflective, self-cleaning, and durable coatings for solar cell applications. *J Coat Technol Res* 21(1):1–30
- Sutar RS, Patil PB, Bhosale AK, Nagappan S, Shinde SR, Chikode PP, Patil CE, Kadam SS, Kadam PM, Bobade CR, Sadasivuni KK (2021) Photocatalytic and Superhydrophilic TiO_2 - SiO_2 Coatings on Marble for Self-Cleaning Applications. *Macromol Symp* 400(1):2100083
- Ren Y, Li W, Cao Z, Jiao Y, Xu J, Liu P, Li S, Li X (2020) Robust TiO_2 nanorods- SiO_2 core-shell coating with high-performance self-cleaning properties under visible light. *Appl Surf Sci* 509:145377
- Kumar A, Nayak D, Nandi BK, Saxena VK, Thangavel R (2023) Visible light active and self-cleaning $\text{SiO}_2/\text{N-TiO}_2$ heterostructure surface with high transmittance for solar module glass cover: Experimental and DFT insights. *J Environ Chem Eng* 11(5):111117
- Yue R, Rahaman MS (2022) Hydrophilic and underwater superoleophobic porous graphitic carbon nitride (g-C₃N₄) membranes with photo-Fenton self-cleaning ability for efficient oil/water separation. *J Colloid Interface Sci* 608:1960–72
- Koysuren O, Dhoska K, Koysuren HN, Markja I, Yaglikci S, Tuncel B, Bebi E (2021) $\text{SiO}_2/\text{WO}_3/\text{ZnO}$ based self-cleaning coatings for solar cells. *J Sol Gel Sci Technol* 110(1):183–203
- Ghamgosar Khorshidi Z, Jallab M, Moghbelli E, Goudarzi A, Ghaffari M (2021) Photocatalytic Analysis of a Hydrophilic Acrylic Coating/Zinc Oxide Nanocomposite on Glass Substrate. *Polym Plast Tech Mater* 60(11):1220–32
- Rudakova AV, Emeline AV, Bulanin KM, Chistyakova LV, Maevskaya MV, Bahnemann DW (2018) Self-cleaning properties of zirconium dioxide thin films. *J Photochem Photobiol A Chem* 367:397–405
- Adachi T, Lathe SS, Gosavi SW, Roy N, Suzuki N, Ikari H, Kato K, Katsumata KI, Nakata K, Furudate M, Inoue T (2018) Photocatalytic, superhydrophilic, self-cleaning TiO_2 coating on cheap, light-weight, flexible polycarbonate substrates. *Appl Surf Sci* 458:917–23
- Rana A, Kumar A, Sharma G, Naushad M, Bathula C, Stadler FJ (2021) Pharmaceutical pollutant as sacrificial agent for sustainable synergistic water treatment and hydrogen production via novel Z-scheme $\text{Bi}_7\text{O}_9\text{I}_3/\text{B}_4\text{C}$ heterojunction photocatalysts. *J Mol Liq* 343:117652
- Cao X, Shang L, Liang Y, Lu Z, Zhang G, Xue Q (2019) Tribological investigation of boron carbide films sliding against different mating materials under high relative humidity. *Ceram Silik* 63:380–389
- Ruiz S, Yoo Y, Wadle L, Chen X, Li N, Lu Y, Wohl CJ, Wiesner V, Cui B (2023) Laser ablative patterning of B_4C and MoAlB ceramics for hydrophobic surfaces. *J Am Ceram Soc* 106(10):5712–5722
- Yan D, Liu J, Fu X, Liu P, Luo HA (2019) Low-temperature synthesis of mesoporous boron carbides as metal-free photocatalysts for enhanced CO_2 reduction and generation of hydroxyl radicals. *J Mater Sci* 54:6151–63
- Koysuren O, Koysuren HN (2022) Preparation and activity evaluation of $\text{B}_4\text{C}/\text{ZnO}$ composite photocatalyst. *J Sol Gel Sci Technol* 103(1):172–84
- Zhang X, Wang L, Du Q, Wang Z, Ma S, Yu M (2016) Photocatalytic CO_2 reduction over $\text{B}_4\text{C}/\text{C}_3\text{N}_4$ with internal electric field under visible light irradiation. *J Colloid Interface Sci* 464:89–95

21. Lv Y, Liu Y, Wei J, Li M, Xu D, Lai B (2021) Bisphenol S degradation by visible light assisted peroxy monosulfate process based on BiOI/B4C photocatalysts with Z-scheme heterojunction. *Chem Eng J* 417:129188
22. Ismail AA, Alzubi F, Al-Hajji LA, Alseidi M, Ahmad S, Alduweesh A (2023) Self-cleaning coatings for minimizing the impact of dust precipitation on the power production of solar cells utilizing mesoporous TiO₂/SiO₂ and ZnO/SiO₂ films. *Ceram Int* 49(14):22788–96
23. Zhang B, Xia R, Yan Y, Liu J, Guan Z (2023) Highly Transparent and Zirconia-Enhanced Sol-Gel Hybrid Coating on Polycarbonate Substrates for Self-Cleaning Applications. *Materials* 16(8):3138
24. Mokhtarifar M, Kaveh R, Bagherzadeh M, Lucotti A, Pedferri M, Diamanti MV (2020) Heterostructured TiO₂/SiO₂/γ-Fe₂O₃/rGO coating with highly efficient visible-light-induced self-cleaning properties for metallic artifacts. *ACS Appl Mater Interfaces* 12(26):29671–83
25. Li Y, Yang K, Xia B, Yang B, Yan L, He M, Yan H, Jiang B (2017) Preparation of mechanically stable triple-layer interference broadband antireflective coatings with self-cleaning property by sol-gel technique. *RSC Adv* 7:14660–14668
26. Qi B, Wang J (2013) Fill factor in organic solar cells. *Phys Chem Chem Phys* 15(23):8972–8982
27. Omotosho KD, Gurung V, Banerjee P, Shevchenko EV, Berman D (2024) Self-Cleaning Highly Porous TiO₂ Coating Designed by Swelling-Assisted Sequential Infiltration Synthesis (SIS) of a Block Copolymer Template. *Polymers* 16(3):308
28. Wang X, Ding H, Lv G, Zhou R, Ma R, Hou X, Zhang J, Li W (2022) Fabrication of superhydrophilic self-cleaning SiO₂-TiO₂ coating and its photocatalytic performance. *Ceram Int* 48(14):20033–20040
29. Kipcak AS, Gurses P, Derun EM, Tugrul N, Piskin S (2013) Characterization of boron carbide particles and its shielding behavior against neutron radiation. *Energy Conv Manag* 72:39–44
30. Wang X, Ding H, Wang C, Zhou R, Li Y, Li W, Ao W (2021) Self-healing superhydrophobic A-SiO₂/N-TiO₂@ HDTMS coating with self-cleaning property. *Appl Surf Sci* 567:150808
31. Hamd SS, Ramizy A, Ismail RA (2022) Preparation of novel B4C nanostructure/Si photodetectors by laser ablation in liquid. *Sci Rep* 12(1):16529
32. Kashif Z, Naz MY, Maqbool A, Shukrullah S, Irfan M, Faraj Mursal SN, Rahman S, Magzoub Mohamed Ali MA (2024) Study of dual Z-scheme photocatalytic response of TiO₂/Ag/ZnO coating on plasma-modified cotton fabric for self-cleaning application. *AIP Adv* 14(1):015222
33. Azleen F, Ratnawulan R, Fauzi A, Rahmadhani D, Steven A, Anisa K (2023) Effect of Composition Variation on The Crystal Size and Band Gap of Thin Film Nano Photocatalyst Fe₂O₃/CuO/MnO₂. *Environ Earth Sci* 1228(1):012017
34. Bledowski M, Wang L, Ramakrishnan A, Khavryuchenko OV, Khavryuchenko VD, Ricci PC, Strunk J, Cremer T, Kolbeck C, Beranek R (2011) Visible-light photocurrent response of TiO₂-polyheptazine hybrids: Evidence for interfacial charge-transfer absorption. *Phys Chem Chem Phys* 13(48):21511–21519
35. Gao HJ, Yang H, Wang SF (2018) Hydrothermal synthesis, growth mechanism, optical properties and photocatalytic activity of cubic SrTiO₃ particles for the degradation of cationic and anionic dyes. *Optik* 175:237–249
36. Wang X, Yang L, Yang DQ, Sacher E (2023) Surface wettability effects on self-cleaning efficacy: Outdoor experimental study. *Sol Energy* 266:112190
37. Dalawai SP, Aly MA, Latthe SS, Xing R, Sutar RS, Nagappan S, Ha CS, Sadasivuni KK, Liu S (2020) Recent advances in durability of superhydrophobic self-cleaning technology: a critical review. *Prog Org Coat* 138:105381
38. Mishra A, Gill FS, Bhatt N, Rathod AP, Rajput A (2024) Fabrication of antireflective superhydrophobic coating for self-cleaning solar panels and study of energy efficiency. *Phys Fluids* 36(1):017111